PNAS RESEARCH ARTICLE | NEUROSCIENCE OPEN ACCESS

EGR4 is critical for cell-fate determination and phenotypic maintenance of geniculate ganglion neurons underlying sweet and umami taste

Debarghya Dutta Banik[a], Louis J. Martin[a], Tao Tang[a], Jonathan Soboloff[b], Warren G. Tourtellotte[c], and Brian A. Pierchala[a,1]

Edited by Robert F. Margolskee, Monell Chemical Senses Center, Philadelphia, PA; received October 17, 2022; accepted March 23, 2023 by Editorial Board Member Jeremy Nathans

The sense of taste starts with activation of receptor cells in taste buds by chemical stimuli which then communicate this signal via innervating oral sensory neurons to the CNS. The cell bodies of oral sensory neurons reside in the geniculate ganglion (GG) and nodose/petrosal/jugular ganglion. The geniculate ganglion contains two main neuronal populations: BRN3A+ somatosensory neurons that innervate the pinna and PHOX2B+ sensory neurons that innervate the oral cavity. While much is known about the different taste bud cell subtypes, considerably less is known about the molecular identities of PHOX2B+ sensory subpopulations. In the GG, as many as 12 different subpopulations have been predicted from electrophysiological studies, while transcriptional identities exist for only 3 to 6. Importantly, the cell fate pathways that diversify PHOX2B+ oral sensory neurons into these subpopulations are unknown. The transcription factor EGR4 was identified as being highly expressed in GG neurons. EGR4 deletion causes GG oral sensory neurons to lose their expression of PHOX2B and other oral sensory genes and up-regulate BRN3A. This is followed by a loss of chemosensory innervation of taste buds, a loss of type II taste cells responsive to bitter, sweet, and umami stimuli, and a concomitant increase in type I glial-like taste bud cells. These deficits culminate in a loss of nerve responses to sweet and umami taste qualities. Taken together, we identify a critical role of EGR4 in cell fate specification and maintenance of subpopulations of GG neurons, which in turn maintain the appropriate sweet and umami taste receptor cells.

taste | chemosensory | cell fate determination | geniculate ganglion | EGR4

Significance

Our understanding of the development and diversification of oral sensory neurons that underly the sense of taste is rudimentary. The oral projecting neurons of the geniculate ganglia (GG) transduce the five taste qualities from their origin in taste buds to the brainstem. The transcriptional regulatory mechanisms underlying diversification of the unique neuronal subpopulations responsive to these stimuli remain elusive. Here, we demonstrate the EGR4, a zinc-finger transcription factor, plays a critical role in cell-fate specification and maintenance of selective subpopulations of GG oral sensory neurons. EGR4 is also required to maintain their proper innervation of taste buds, as well as the corresponding taste bud cell subtypes that underlie sweet and umami taste qualities.

The combinatorial action of neurotrophic factors, signal transduction pathways, transcription factors, and synaptic complexes determines the cellular identity of sensory neurons during the development of the nervous system (1). Transcription factors often modulate the expression of additional transcriptional modulators, neurotransmitter receptors, neurotransmitter synthesis pathways, neuropeptides, and other genes that define the molecular and functional characteristics of distinct subpopulations of sensory neurons, and this has been well established in dorsal root ganglia (DRG) (2–5). The geniculate ganglion (GG) is well suited for the study of development, diversification, and maintenance of distinct populations of neurons because it consists of heterogenous sensory neurons transducing different sensory modalities including taste, temperature, and touch. The GG is composed of two primary populations of neurons: 1) oral sensory neurons that transduce taste, thermal, and somatosensory information from the oral cavity and 2) somatosensory neurons that innervate the pinna or outer ears. A transcriptional profile of *Islet1+/Phox2b+/Brn3a-* defines the oral sensory neuronal fate, whereas an *Islet1+/Phox2b-/Brn3a+* combination delineates the pinna somatosensory fate (6). However, the molecular mechanisms directing cell fate specification and maintenance of the subpopulations within these two main classes of neurons remain poorly understood.

Previous studies have identified several subpopulations of GG oral sensory neurons unique for their responses to taste and sensory modalities. One of these studies identified a *Ret+* subpopulation of oral sensory neurons that are mechanoreceptors (7). A second study using single-cell RNA-seq (scRNA-seq) found three main subpopulations of PHOX2B+ oral sensory neurons which were *Foxg1+, Trhr+, and Mafb+* (8). An additional scRNA-seq analysis identified six subpopulations of oral sensory neurons in which five were selectively responsive to each of the five taste qualities (*Cdh4+, Cdh13+, Egr2+, Spon1+, and Penk+*) and the sixth was most likely mechanosensory (*Piezo2+*) (9). Although these studies have begun to unravel the diversity of GG oral sensory neurons, the transcriptional mechanisms and signaling pathways that give rise to these distinct subpopulations of neurons are not known.

Author contributions: D.D.B. and B.A.P. designed research; D.D.B., L.J.M., and T.T. performed research; J.S. and W.G.T. contributed new reagents/analytic tools; J.S. provided the Egr4$^{-/-}$ mice; D.D.B., L.J.M., T.T., and B.A.P. analyzed data; and D.D.B., L.J.M., T.T., and B.A.P. wrote the paper.

The authors declare no competing interest.

This article is a PNAS Direct Submission. R.F.M. is a guest editor invited by the Editorial Board.

[1]To whom correspondence may be addressed. Email: brpierch@iu.edu.

This article contains supporting information online at https://www.pnas.org/lookup/suppl/doi:10.1073/pnas.2217595120/-/DCSupplemental.

Published May 22, 2023.

GG oral sensory neurons innervate taste buds of fungiform papillae and taste buds located in the upper palate of the oral cavity. Taste buds house a heterogeneous group of taste receptor cells that detect different taste qualities and transduce this information via GG oral sensory neurons to the CNS. Taste receptor cells and the supporting cells have a limited lifespan of 8 to 12 d on average before being replaced by newly differentiated cells (10–12). These differentiated cells originate from Keratin14+ progenitor cells that become either nontaste epithelium or postmitotic precursors that express Sonic Hedgehog (SHH). These SHH+ cells further differentiate into functional taste bud cells. Gustatory neuronal input has long been identified as a necessary factor for taste bud maintenance and taste bud cell replenishment since adult taste buds disintegrate after their nerve supply is disrupted (13–16), and taste bud restoration only occurs after reinnervation by GG neurons (17, 18). It has been suggested that neuron-supplied factors regulate adult taste progenitor cell activity and recent studies identified *Sonic hedgehog* (*Shh*) and *R-spondin2* as important neuron-supplied factors for taste bud maintenance and regeneration (19, 20), although epithelial Shh is sufficient for maintenance of taste buds (21). However, the extent to which GG innervation selectively regulates the development or maintenance of any specific taste cell population is not known.

To better understand the active transcriptional profile of GG oral sensory neurons, we used ribosomal profiling to explore oral sensory neuron-specific gene expression in vivo using a *Phox2b*-driven Ribotag mouse model (22, 23). Interestingly, early growth response protein 4 (*Egr4*), a transcription factor belonging to the EGR family of zinc-finger transcription factors, was found to be highly enriched in PHOX2B+ GG oral sensory neurons. Using fluorescence in situ hybridization (FISH) and immunolabeling, we show that both *Egr4* mRNA and EGR4 protein are highly expressed in GG neurons by postnatal day 30. Deletion of *Egr4* causes a significant loss of PHOX2B+ GG oral sensory neurons with a concomitant increase in BRN3A+ neurons, without affecting neuronal survival. Consistent with an observed decrease in chemosensory innervation of taste buds in both fungiform and Circumvallate papillae, nerve responses to sweet and umami tastants are significantly reduced in $Egr4^{-/-}$ mice. Finally, RNA-seq analysis indicated that EGR4 regulates the expression of axon guidance and synaptogenesis proteins in both GG neurons and axon terminals innervating taste buds, likely resulting in the observed innervation deficits. These data indicate that EGR4 is involved in cell-fate determination of GG neurons, as well as maintenance of bud innervation, likely by modulating axon guidance and synaptogenesis.

Results

***Egr4* mRNA and Protein Expression in Geniculate Ganglion and Nodose/Petrosal Ganglion.** Transcriptional profiling of PHOX2B+ GG neurons identified the transcription factor *Egr4* as highly enriched in *Phox2b*-expressing GG neurons as compared to total GG mRNA (eightfold enriched). To determine when, and to what extent, *Egr4* mRNA is expressed in individual GG neurons, we utilized FISH (Fig. 1*A*). *Egr4* mRNA was highly expressed in both *Phox2b*+ oral sensory and *Brn3a*+ somatosensory neurons of adult GG (P30). *Egr4* mRNA, however, was not expressed prior to postnatal day 7 (P7) and was not highly expressed until postnatal day 10 (P10) (Fig. 1*A*). To corroborate the FISH expression of *Egr4*, we utilized immunolabeling to evaluate the expression of EGR4 protein in GG neurons (Fig. 1*B*). We found the same EGR4 expression pattern that was observed with FISH in which EGR4 protein is widespread in all GG neurons in adulthood but is not present before P7. When we analyzed the total number and proportion of PHOX2B+ oral sensory neurons in the GG across postnatal age, we did not find any differences (Fig. 1*C* and *SI Appendix*, Fig. S1*A*, respectively). We next analyzed the total number of EGR4+ neurons and their proportion to TUJ1+ neurons in the GG over these ages (Fig. 1*D* and *SI Appendix*, Fig. S1*B*, respectively). We also analyzed the total number of neurons that co-express PHOX2B and EGR4 and what proportion of PHOX2B+ neurons express EGR4 (Fig. 1*E* and *SI Appendix*, Fig. S1*C*, respectively). Higher magnification (63×) images of the P30 GG FISH experiment revealed two populations of *Egr4*+*Phox2b* neurons. One population has higher expression of *Egr4* mRNA (marked by white arrowhead), whereas the other population has low *Egr4* mRNA (yellow arrowhead) expression (*SI Appendix*, Fig. S1*D*). Nevertheless, all *Phox2b*+ neurons express *Egr4* mRNA. We also investigated EGR4 expression in Nodose/Petrosal ganglia which innervates the circumvallate papillae via glossopharyngeal nerve (*SI Appendix*, Fig. S1*E*) (24). We found that EGR4 protein is widely expressed in PHOX2B+ Nodose/Petrosal chemosensory neurons as well in some PHOX2B- neurons as well. Together, these results indicate that *Egr4* mRNA and EGR4 protein start to be expressed between postnatal days 3 and 7 and become widely expressed in all GG neurons by P30, irrespective of whether it is an oral sensory or pinna somatosensory neuron. We also analyzed EGR4 immunolabeling intensity (as a proxy of protein level) and found that it is significantly higher in PHOX2B+ neurons, as compared to PHOX2B- pinna-projecting neurons, which matches the ribosomal profiling data (Fig. 1*F*).

EGR4 Is Essential in Maintaining Homeostasis in the Ratio of Oral Cavity-Projecting and Pinna-Projecting Neurons in the Geniculate Ganglion. Sensory neuron diversification depends on differential transcriptional activities that induce and maintain expression of required growth factor receptors, which in turn serve phenotypic activator or repressor functions (3). GG neurons begin their transcriptional fate acquisition and initial axon outgrowth from E12.5 to E14.5 (6), but the process of reaching their final targets is not completed until near birth (25). As EGR4 is not expressed until postnatal days 3–7, we hypothesized that EGR4 is required to maintain the initial differentiation of oral sensory neurons of the GG. To evaluate this, we analyzed the number of GG neurons and PHOX2B+ oral sensory neurons in $Egr4^{-/-}$ mice, or $Egr4^{+/+}$ mice as a control, at P30 (Fig. 2*A*) (26). Although there was no difference in total number of neurons (Fig. 2*B*), there was a significant reduction in the total number and proportion of neurons that were PHOX2B+ (Fig. 2 *C* and *D* respectively). Quantification of the intensity of TUJ1+ labeling, as well as PHOX2B labeling indicated a substantial reduction in both. (Fig. 2 *E* and *F*).

Since EGR4 is also expressed in neurons expressing the pinna somatosensory transcriptional fate determinant BRN3A (27), we investigated whether the loss of PHOX2B expression was coupled with a change in the proportion of the BRN3A+ neurons. There was a striking increase in both the BRN3A+ somatosensory neurons and their proportion in the GG with the concomitant decrease in the proportion of the PHOX2B+ neurons (Fig. 2 *G*–*L*). To corroborate our immunolabeling result, we performed FISH labeling using *Phox2b* and *Brn3a* mRNA probes (*SI Appendix*, Fig. S2). This experiment confirmed the loss of *Phox2b* expression and a simultaneous increase in *Brn3a* mRNA expression in GG neurons from $Egr4^{-/-}$ mice compared to $Egr4^{+/+}$ mice. These data suggest that EGR4 is essential for maintaining the expression of PHOX2B in oral sensory neurons and that in its absence, BRN3A expression is up-regulated, increasing somatosensory phenotype of GG neurons.

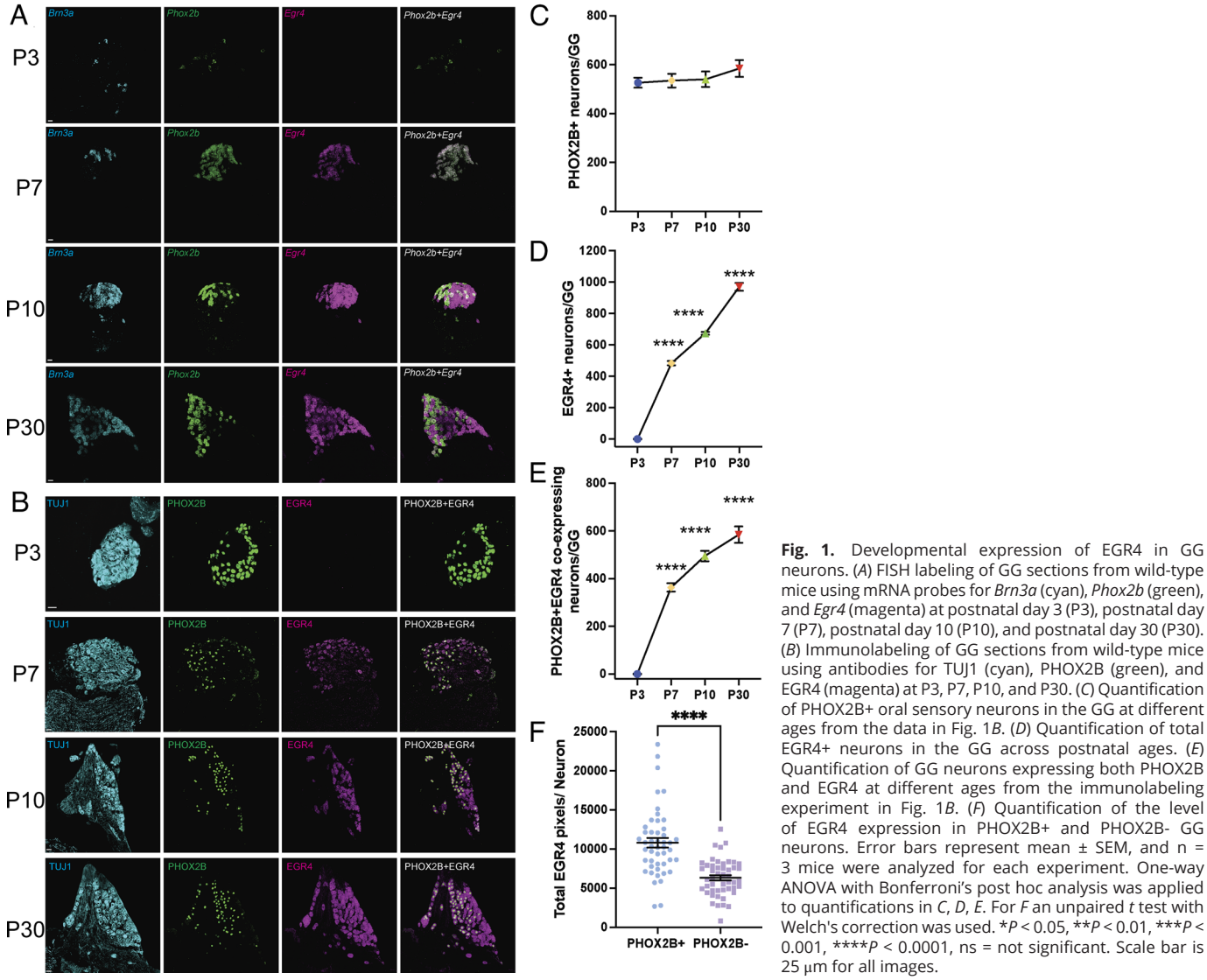

Fig. 1. Developmental expression of EGR4 in GG neurons. (*A*) FISH labeling of GG sections from wild-type mice using mRNA probes for *Brn3a* (cyan), *Phox2b* (green), and *Egr4* (magenta) at postnatal day 3 (P3), postnatal day 7 (P7), postnatal day 10 (P10), and postnatal day 30 (P30). (*B*) Immunolabeling of GG sections from wild-type mice using antibodies for TUJ1 (cyan), PHOX2B (green), and EGR4 (magenta) at P3, P7, P10, and P30. (*C*) Quantification of PHOX2B+ oral sensory neurons in the GG at different ages from the data in Fig. 1*B*. (*D*) Quantification of total EGR4+ neurons in the GG across postnatal ages. (*E*) Quantification of GG neurons expressing both PHOX2B and EGR4 at different ages from the immunolabeling experiment in Fig. 1*B*. (*F*) Quantification of the level of EGR4 expression in PHOX2B+ and PHOX2B- GG neurons. Error bars represent mean ± SEM, and n = 3 mice were analyzed for each experiment. One-way ANOVA with Bonferroni's post hoc analysis was applied to quantifications in *C*, *D*, *E*. For *F* an unpaired *t* test with Welch's correction was used. $^{*}P < 0.05$, $^{**}P < 0.01$, $^{***}P < 0.001$, $^{****}P < 0.0001$, ns = not significant. Scale bar is 25 μm for all images.

Loss of EGR4 Impacts Several Subpopulations of PHOX2B+ Oral Sensory Neurons in the GG. Previous studies have identified several subpopulations of PHOX2B+ oral sensory neurons in the GG. One study identified three subpopulations which are distinguished by expression of *Mafb*, *Foxg1*, and *Trhr* (8). A second study identified 6 subpopulations distinguished by the selective expression of *Cdh4, Cdh13, Egr2, Spon1, Penk*, and *Piezo2* (9). Since the loss of EGR4 significantly reduced PHOX2B expression, we investigated how these subpopulations were affected by the loss of EGR4. Immunolabeling experiments revealed a significant loss of MAFB+ neurons and their proportion in the GG of $Egr4^{-/-}$ mice compared to $Egr4^{+/+}$ mice (Fig. 3 *A*–*C*). MAFB is typically expressed in mechanosensory neurons, as is *Ret*, and the number and proportion of *Ret*+ mechanosensory neurons were examined accordingly. *Ret*+ neurons and their proportion were also significantly reduced in $Egr4^{-/-}$ GG compared to wild-type littermates (Fig. 3 *D*–*F*). We next investigated FOXG1 expression in the GG of $Egr4^{-/-}$ mice as compared to $Egr4^{+/+}$ mice (Fig. 3 *G*–*I*) and found a significant reduction in the number of FOXG1+ neurons and their proportion in $Egr4^{-/-}$ GG. Several attempts were made to visualize the third subpopulation of oral sensory neurons described in Dvoryanchikov et al. study, *Trhr*+ neurons, using TRHR antibodies and *Trhr* FISH probes, but we were unable to achieve subpopulation-specific labeling. Four subpopulations described in the Zhang et.al. study were evaluated with mRNA probes, the genes *Cdh13*, *Penk, Spon1, and Cdh4.* We found a significant reduction in the number of *Cdh13*+ neurons but no change in the number of *Penk*+ neurons (Fig. 3 *J*–*M*). Interestingly, a small population of neurons that expressed both *Cdh13* and *Penk* was observed, and this population was not affected by the loss of EGR4 (marked by white arrowhead). Likewise, we also found significant reduction in the number of both *Spon1*+ and *Cdh4*+ neurons (Fig. 3 *N*–*Q*). We also found a population of neurons which coexpressed both *Spon1* and *Cdh4.* This population was not affected by the loss of EGR4 (marked by white arrowhead). Taken together, these data suggest that although the loss of EGR4 significantly affects PHOX2B+ oral sensory neurons, not all subpopulations are affected in $Egr4^{-/-}$ mice.

EGR4 Deletion Causes in a Reduction in Taste Bud Number, Size, and Chemosensory Innervation in Fungiform Papillae. Since EGR4 is required to maintain homeostasis between the oral sensory and pinna somatosensory phenotypes in the postnatal GG, and loss of EGR4 causes a switch from PHOX2B+ to BRN3A+ neurons, we hypothesized that loss of EGR4 would also disrupt chemosensory innervation of fungiform taste buds. Anterior tongues were collected from $Egr4^{+/+}$ and $Egr4^{-/-}$ mice at four different ages: P3 (when EGR4 is not expressed in GG neurons), P7 (initiation of EGR4 expression),

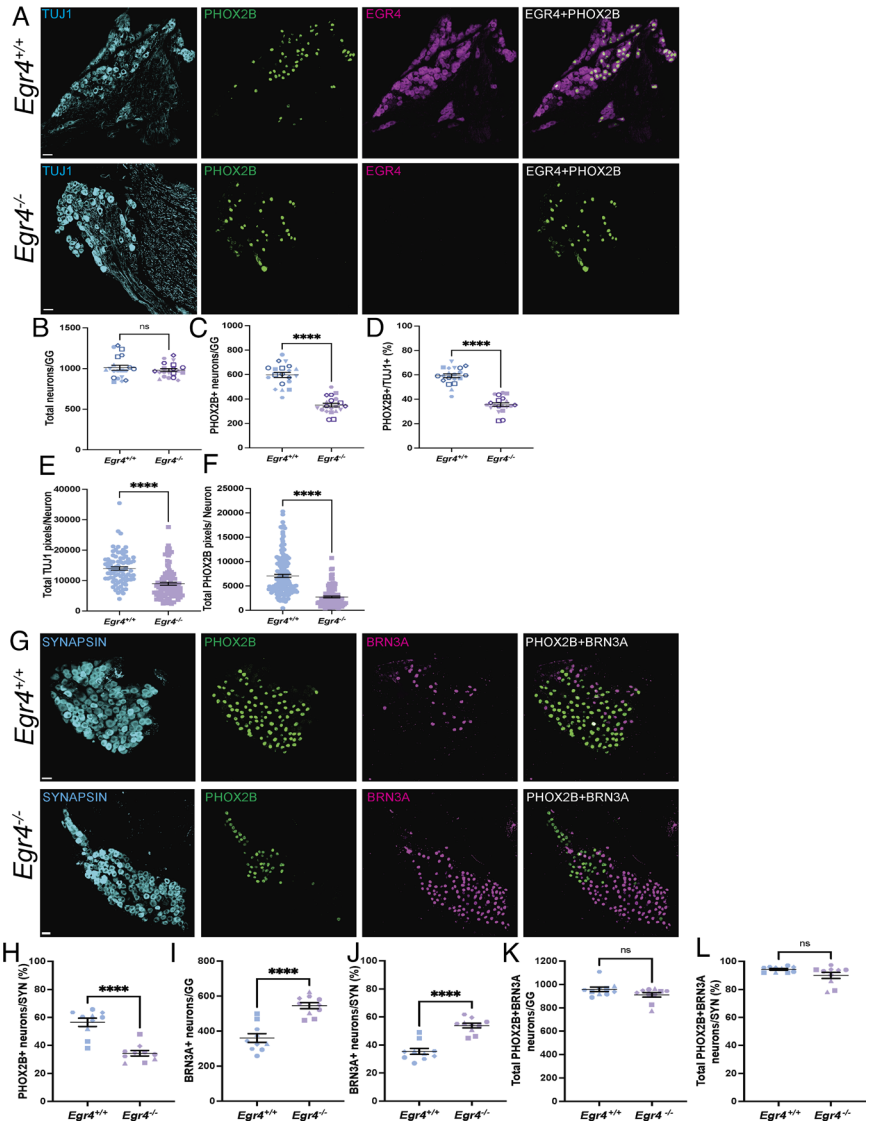

Fig. 2. PHOX2B+ oral sensory neurons decline with a concomitant increase in BRN3A+ somatosensory neurons in GG of *Egr4*$^{-/-}$ mice. (*A*) Immunolabeling of GG neurons using antibodies against TUJ1 (cyan), PHOX2B (green), and EGR4 (magenta). The *Top* panels show GG sections from *Egr4*$^{+/+}$ mice, and the *Lower* panels are GG sections from *Egr4*$^{-/-}$ mice. (*B*) The total number of neurons (TUJ1+) in each ganglion were analyzed from *Egr4*$^{+/+}$ and *Egr4*$^{-/-}$ mice and quantified. (*C*) The total number of PHOX2B+ oral sensory neurons and (*D*) the proportion of the oral sensory neurons out of total neurons, were also quantified between *Egr4*$^{+/+}$ and *Egr4*$^{-/-}$ mice. (*E*) Total TUJ1 pixels per GG neuron was measured between *Egr4*$^{+/+}$ and *Egr4*$^{-/-}$ mice. (*F*) The amount of PHOX2B pixels per neuron was quantified between *Egr4*$^{+/+}$ and *Egr4*$^{-/-}$ mice. (*G*) Immunolabeling of GG neurons using antibodies against SYNAPSIN (cyan), PHOX2B (green), and BRN3A (magenta). The *Top* panels are representative GG sections from *Egr4*$^{+/+}$ mice, and the lower panels are GG sections from *Egr4*$^{-/-}$ mice. (*H*) The percentage of PHOX2B+ oral sensory neurons out of the total number of neurons was analyzed between the *Egr4*$^{+/+}$ and *Egr4*$^{-/-}$ mice. (*I*) The total number of BRN3A+ somatosensory neurons, and (*J*) the proportion of the BRN3A+ somatosensory neurons as compared to the total number of neurons were analyzed between the *Egr4*$^{+/+}$ and *Egr4*$^{-/-}$ mice. (*K*) The total number of PHOX2B+ and BRN3A+ neurons together and (*L*) their proportion out of total neurons were also compared between the *Egr4*$^{+/+}$ and *Egr4*$^{-/-}$ mice. Error bars represent mean ± SEM, n = 5 to 10. An unpaired *t* test with Welch's correction was used. **P* < 0.05, ***P* < 0.01, ****P* < 0.001, *****P* < 0.0001, ns = not significant. Scale bar is 25 μm for all images, and all mice were P30.

P10 (greater EGR4 expression), and P30 (when all neurons in the GG express EGR4) (Fig. 4*A*). The tongues were immunolabeled for K8 (taste cell marker), TUJ1 (pan-neuronal marker), and P2X3 (chemosensory nerve fiber marker) and the following anatomic structures were analyzed: 1) Total taste bud number, 2) Taste bud area, 3) Total K8 pixels/taste bud, 4) Total TUJ1 pixels/taste bud, and 5) Total P2X3 pixels/taste bud. (Fig. 4 *B–J*). There were no differences in any of the criteria analyzed between *Egr4*$^{+/+}$ and *Egr4*$^{-/-}$ mice at P3. However, there were significant differences in all measurements in *Egr4*$^{-/-}$ mice at P7, P10, and P30 when compared to *Egr4*$^{+/+}$ littermates. Summary of the data is included in *SI Appendix*, Table S1.

During this investigation, we found several fungiform papillae that did not contain a taste bud but still had nerve fiber innervation (labeled by TUJ1) without apparent chemosensory fibers (marked by P2X3) (*SI Appendix*, Fig. S3*A*). On further analysis, these papillae lacking taste buds were far more abundant in *Egr4*$^{-/-}$ mice than *Egr4*$^{+/+}$ mice (*SI Appendix*, Fig. S3*B*). It is possible that these papillae housed a taste bud initially, but the loss of innervation in *Egr4*$^{-/-}$ mice caused the subsequent loss of the taste bud, followed by the almost complete loss of chemosensory fibers. The remaining TUJ1+ fibers may be extragemmal somatosensory fibers. Alternatively, the remaining TUJ1+ fibers may have initially been P2X3+ as well but eventually lost P2X3 expression over time in the absence of EGR4.

***Egr4*$^{-/-}$ Mice Have a Reduction in Taste Bud Number and Chemosensory Innervation of Circumvallate Papillae but Not in the Size of the Taste Bud.** Since EGR4 is expressed in Nodose/Petrosal ganglia, the deficits we observed in fungiform taste buds raised the question of whether similar abnormalities are present in taste bud populations in other regions of the tongue. We chose to examine circumvallate (CV) taste buds in the posterior tongue which are not innervated by oral sensory neurons of the GG and instead are innervated by oral sensory neurons of the petrosal ganglion (24). To evaluate the morphology of the taste buds in CV papillae, posterior tongues were collected from *Egr4*$^{+/+}$ and *Egr4*$^{-/-}$ mice at four different ages: postnatal days 3, 7, 10, and 30, as was done for fungiform papillae. Tongues were immunolabeled for K8, TUJ1, and P2X3, and the same structures were analyzed (*SI Appendix*, Fig. S4 *A–I*). We did not observe any differences in CV taste buds between *Egr4*$^{+/+}$ and *Egr4*$^{-/-}$ mice at P3. However, there were significant differences in total number of taste buds, total K8 pixels/taste bud, total TUJ1 pixels/taste bud, and total P2X3 pixels/taste bud between *Egr4*$^{-/-}$ and *Egr4*$^{+/+}$ mice at P7, P10, and P30. Interestingly, unlike fungiform papillae, we did not observe any difference in CV taste bud area at any age between the Egr4$^{+/+}$ and *Egr4*$^{-/-}$ mice. A summary of the data is included in *SI Appendix*, Table S2.

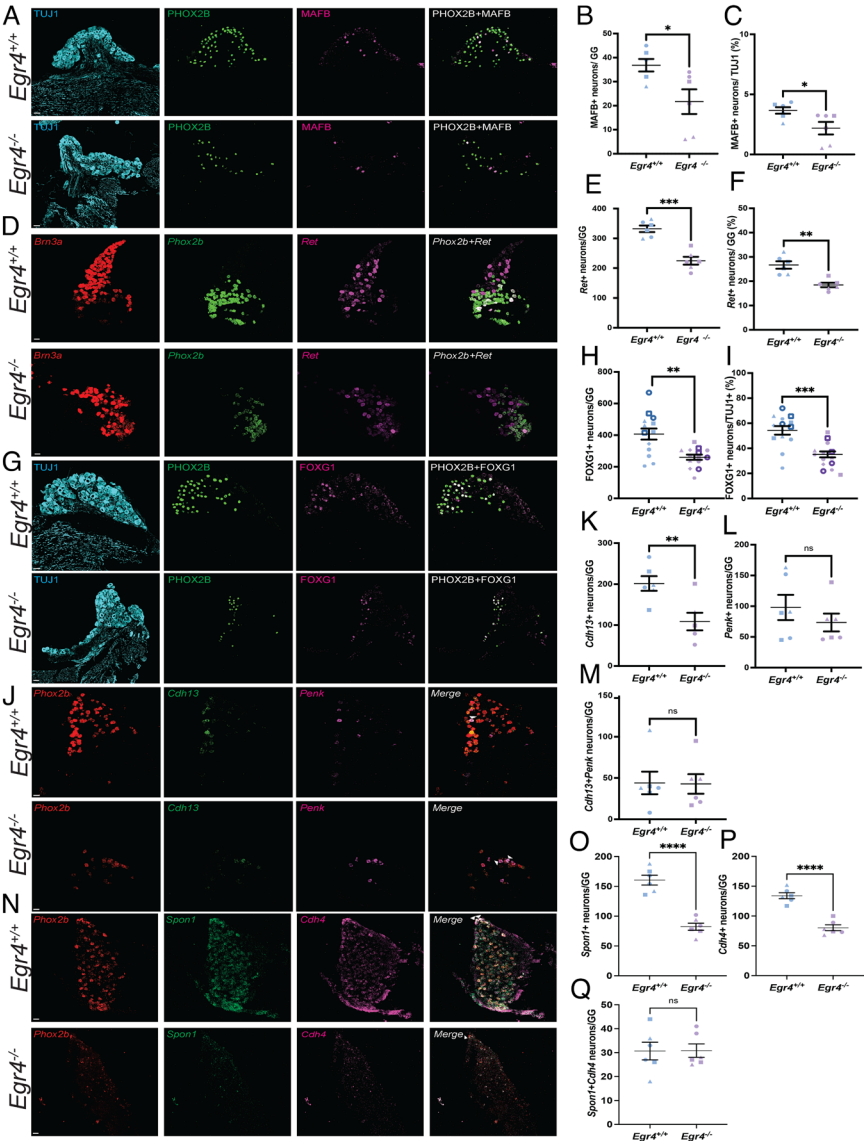

Fig. 3. Subpopulations of the oral sensory neurons of the GG are differentially affected by the loss of EGR4. We evaluated 7 different markers of known subpopulations of oral sensory neurons: MAFB, *Ret*, FOXG1, *Cdh13, Penk, Spon1,* and *Cdh4*. (*A*) Immunolabeling of GG sections using antibodies against TUJ1 (cyan), PHOX2B (green), and MAFB (magenta). The *Top* and *Bottom* panels depict GG sections from *Egr4*$^{+/+}$ and *Egr4*$^{-/-}$ mice, respectively. (*B*) The total number of MAFB+ neurons and (*C*) the percentage of the MAFB+ neurons from total neurons (TUJ1+) were quantified. (*D*) FISH labeling of GG sections using mRNA probes for *Brn3a* (red), *Phox2b* (green), and *Ret* (magenta). The *Top* and *Bottom* panels depict GG sections from *Egr4*$^{+/+}$ and *Egr4*$^{-/-}$ mice, respectively. (*E*) The total number of *Ret*+ neurons, and (*F*) the percentage of the *Ret*+ neurons from total neurons were analyzed between *Egr4*$^{+/+}$ and *Egr4*$^{-/-}$ mice. (*G*) Immunolabeling of GG sections using antibodies against TUJ1 (Cyan), PHOX2B (Green), and FOXG1 (Magenta). The *Top* and *Bottom* panels show sections of GG from *Egr4*$^{+/+}$ and *Egr4*$^{-/-}$ mice, respectively. (*H*) The total number of FOXG1+ neurons, and (*I*) the percentage of the FOXG1+ neurons from total neurons (TUJ1+) were quantified between *Egr4*$^{+/+}$ and *Egr4*$^{-/-}$ mice. (*J*) FISH labeling of GG sections using mRNA probes for *Phox2b* (red), *Cdh13* (green), and *Penk* (magenta). The *Top* and *Bottom* panels show sections of GG from *Egr4*$^{+/+}$ and *Egr4*$^{-/-}$ mice, respectively. (*K*) The total number of *Cdh13*+ neurons, and (*L*) the total number of *Penk*+ neurons were quantified. Some neurons express both *Cdh13* and *Penk* in both *Egr4*$^{+/+}$ and *Egr4*$^{-/-}$ GG (marked by white arrowhead). (*M*) The total number of neurons that express both *Cdh13* and *Penk* were also counted from both *Egr4*$^{+/+}$ and *Egr4*$^{-/-}$ mice. (*N*) FISH labeling of GG sections using mRNA probes for *Phox2b* (red), *Spon1*(green), and *Cdh4* (magenta). The *Top* and *Bottom* panels show sections of GG from *Egr4*$^{+/+}$ and *Egr4*$^{-/-}$ mice, respectively. (*O*) The total number of *Spon1*+ neurons, and (*P*) the total number of *Cdh4*+ neurons were quantified. Some neurons express both *Spon1* and *Cdh4* in both *Egr4*$^{+/+}$ and *Egr4*$^{-/-}$ GG (marked by white arrowhead). (*Q*) The total number of neurons that express both *Spon1* and *Cdh4* were also counted from both *Egr4*$^{+/+}$ and *Egr4*$^{-/-}$ mice. Error bars represent mean ± SEM, and n = 3 to 7 mice. An unpaired *t* test with Welch's correction was applied to these quantifications. **P* < 0.05, ***P* < 0.01, ****P* < 0.001, *****P* < 0.0001, ns = not significant. Scale bar is 25 μm for all images, and mice were P30.

Loss of EGR4 Affects Type I and II Taste Cells but Not Type III Taste Cells. Because we observed a loss of K8 expression in both fungiform and CV taste buds in *Egr4*$^{-/-}$ mice, individual taste cell subpopulations were examined at P30. Taste buds are composed of three main cell types based on morphology: type I, type II, and type III taste cells (28, 29). Type I cells are thin and often partially wrap other taste bud cells and have been suggested to have glial-like function (30). Type II cells express the known receptors for bitter, sweet, and umami compounds and detect these compounds using a G-protein coupled receptor-based signaling mechanism. On the other hand, type III cells are wider than type I and II cells and have traditional chemical synapses. There was a significant increase in the type I taste cell marker nucleoside triphosphate diphosphohydrolase 2 (NTPDASE2) (31) in both fungiform and circumvallate taste papillae in P30 *Egr4*$^{-/-}$ mice compared to *Egr4*$^{+/+}$mice (Fig. 5 *A* and *H* respectively). We were unable to count the number of NTPDASE2+ cells because their elongated shape and intermingled nature made it impossible to tell one cell from the other. As an alternative, the total number of NTPDASE2+ pixels was measured in each taste bud, and a significant increase in the NTPDASE2+ pixels was observed in both fungiform and circumvallate taste buds in *Egr4*$^{-/-}$ mice (Fig. 5 *C* and *J* respectively).

We next investigated how loss of EGR4 affects type II and III taste cells. There was a significant reduction in the type II cell marker transient receptor potential melastatin 5 (TRPM5) (32, 33) in both fungiform and circumvallate taste buds in P30 *Egr4*$^{-/-}$ mice as compared to *Egr4*$^{+/+}$ mice (Fig. 5 *B* and *I* respectively). We analyzed the total number and proportion of TRPM5+ cells, as well as the total TRPM5 pixels (Fig. 5 *D* and *E* and *SI Appendix*, Fig. S5*A* for fungiform and Fig. 5 *K* and *L* and *SI Appendix*, Fig. S5*C* for circumvallate). All these measures were significantly reduced in *Egr4*$^{-/-}$ mice compared to *Egr4*$^{+/+}$ mice. To examine type III taste cells, we used the type III cell marker carbonic anhydrase 4 (CAR4) (34) (Fig. 5 *B* and *I* respectively). Interestingly, there was no difference in the number or proportion of type III cells. CAR4 pixels were also quantified in both fungiform and circumvallate taste buds between *Egr4*$^{-/-}$ and *Egr4*$^{+/+}$ mice, and no significant differences were observed (Fig. 5 *F* and *G* and *SI Appendix*, Fig. S5*B* for fungiform, and Fig. 5 *M* and *N* and *SI Appendix*, Fig. S5*D* for circumvallate). These data suggest that EGR4 is required in GG neurons to maintain TRPM5 expression in type II taste cells.

EGR4 Is Required for Proper Geniculate Ganglion Neuron Responses to Sweet and Umami Taste Qualities. Because of the deficits in GG neurons and taste buds in *Egr4*$^{-/-}$ mice, we evaluated

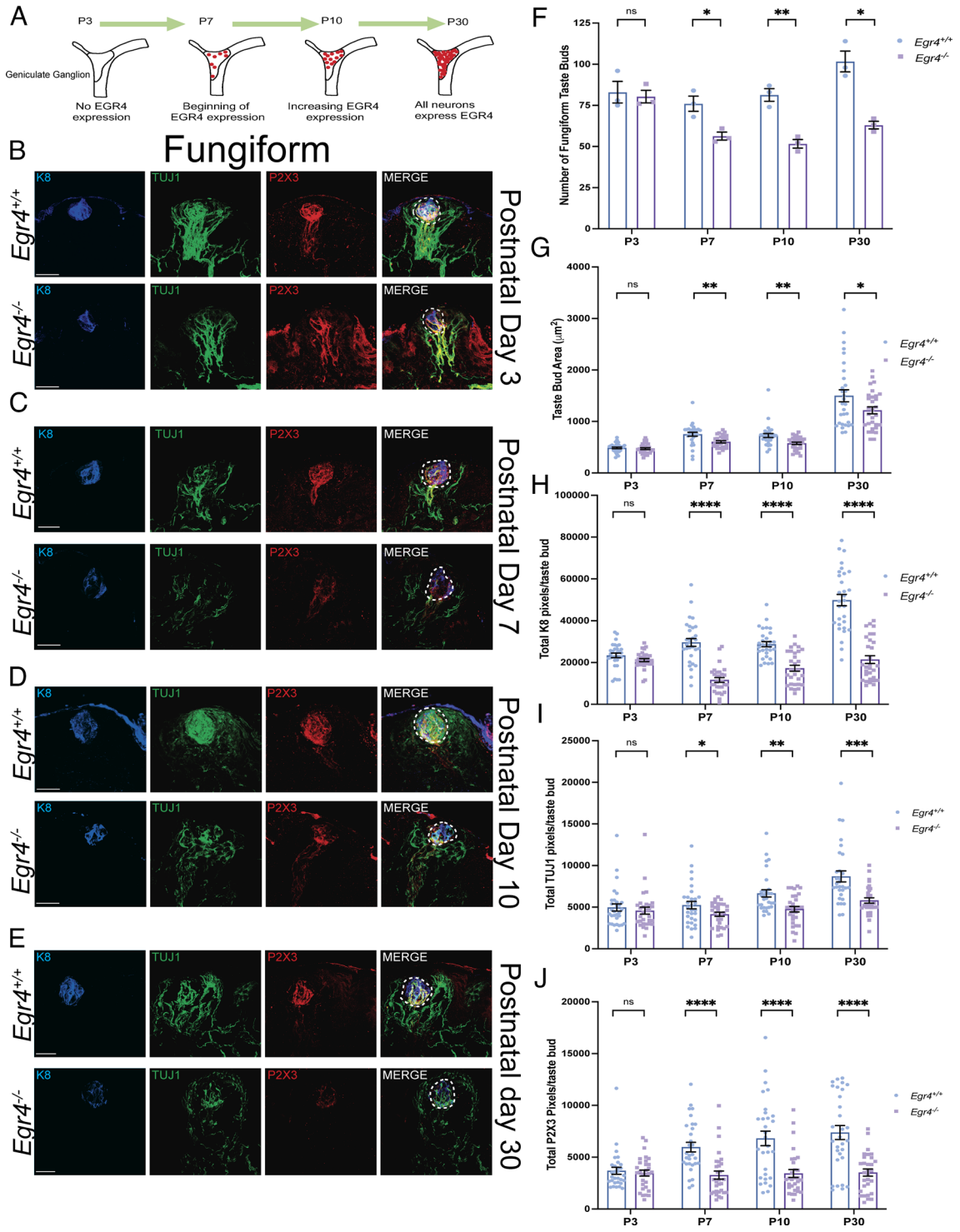

Fig. 4. EGR4 is required for the development and innervation of fungiform taste buds. Loss of EGR4 causes a reduction in the total number of taste buds, taste bud area, and taste bud innervation starting at P7. (*A*) Schematic diagram showing the four different ages from which fungiform papillae were evaluated based on EGR4 expression in GG neurons. (*B*) Fungiform taste buds from *Egr4*$^{+/+}$ (*Top*) and *Egr4*$^{-/-}$ (*Bottom*) mice at P3 were immunolabeled with the taste bud cell marker K8 (blue), pan neuronal marker TUJ1 (green), and chemosensory neuron marker P2X3 (red). (*C*) Fungiform taste buds at P7, (*D*) P10, and (*E*) P30 were immunolabeled with K8 (blue), TUJ1 (green), and P2X3 (red). At each of these ages, the *Top* and *Bottom* panels are fungiform taste buds from *Egr4*$^{+/+}$ and *Egr4*$^{-/-}$ mice, respectively. (*F*) The total number of taste buds, (*G*) taste bud area, and (*H*) total K8 labeling (in pixels) from each taste bud were quantified across ages from both *Egr4*$^{+/+}$ and *Egr4*$^{-/-}$ mice. (*I*) Pan neuronal marker (TUJ1), and (*J*) the chemosensory innervation marker P2X3 in taste buds were also evaluated from the *Egr4*$^{+/+}$ and *Egr4*$^{-/-}$ mice at the different ages. Error bars represent mean ± SEM, n = 3 mice were analyzed. An unpaired *t* test with Welch's correction was applied to these quantifications. *P < 0.05, **P < 0.01, ***P < 0.001, ****P < 0.0001, ns = not significant. Scale bar is 25 μm for all images.

whether lingual sensory deficits are also present by performing whole-nerve recording from the chorda tympany (CT) nerve of *Egr4*$^{+/+}$ and *Egr4*$^{-/-}$ mice. GG oral sensory neurons project to fungiform taste buds via the CT nerve, and these recordings are an assessable means of measuring responses to taste stimuli applied to the anterior tongue. There were no significant differences in neural responses evoked by bitter (quinine), sour (citric acid), salty (NaCl), or amiloride-insensitive NaCl stimuli between *Egr4*$^{-/-}$ and *Egr4*$^{+/+}$ littermates (Fig. 6 *A*, *B*, and *E*–*G*). Amiloride-sensitive NaCl responses were also evaluated and there were no differences

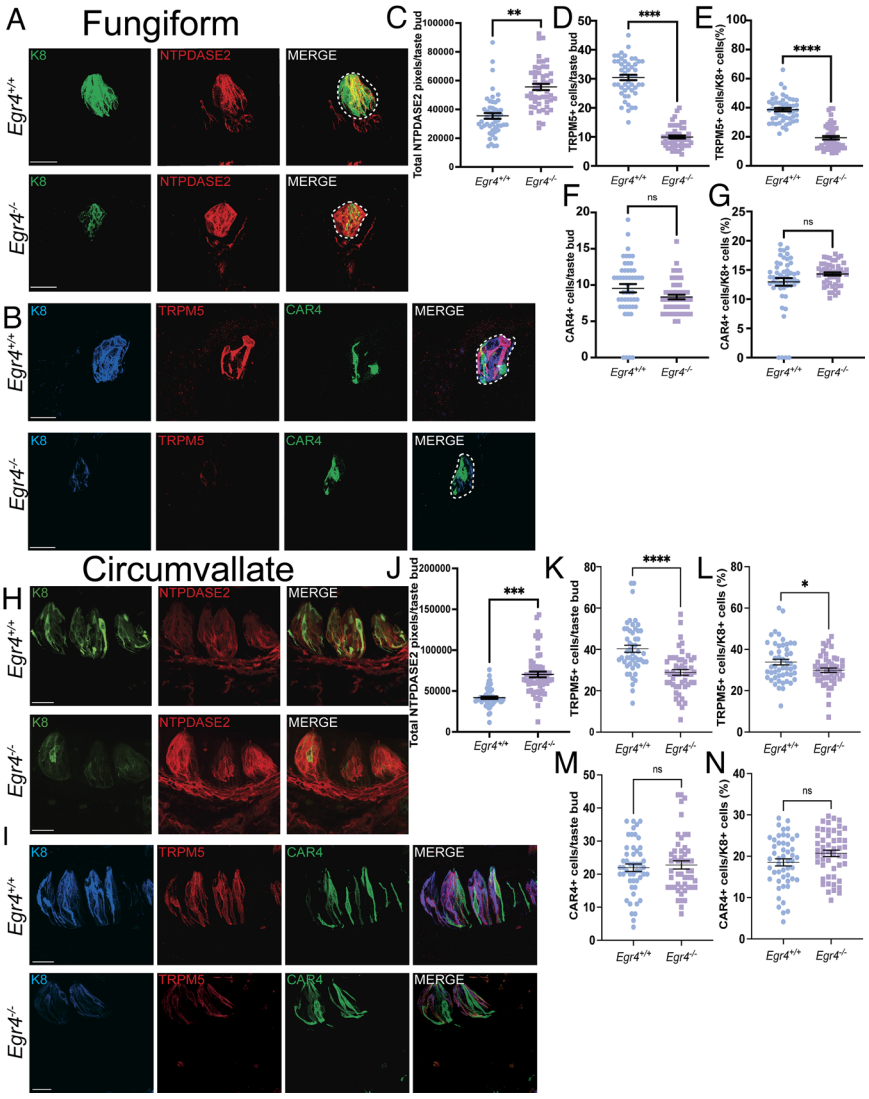

Fig. 5. *Egr4* deletion impacts TRPM5-expressing taste bud cells. (*A*) Fungiform taste buds from *Egr4*$^{+/+}$ (*Top*) and *Egr4*$^{-/-}$ (*Bottom*) at P30 were immunolabeled with the antibodies against K8 (green) and the type I taste bud cell marker NTPDASE2 (red). (*B*) Fungiform taste buds from *Egr4*$^{+/+}$ (*Top*) and *Egr4*$^{-/-}$ (*Bottom*) at P30 were immunolabeled with the antibodies to K8 (blue), the type II taste bud cell marker TRPM5 (red), and the type III taste bud cell marker CAR4 (green). (*C*) Total NTPDASE2+ pixels were significantly increased in *Egr4*$^{-/-}$ taste buds compared to *Egr4*$^{+/+}$ taste buds. (*D*) The total number of TRPM5+ taste bud cells, and (*E*) the proportion of TRPM5+ taste bud cells compared to K8+ taste cells were significantly reduced in the *Egr4*$^{-/-}$ mice as compared to *Egr4*$^{+/+}$ mice. (*F*) The total number of CAR4+ taste bud cells and (*G*) the percentage of the CAR4+ taste bud cells, as compared to all cells in taste buds (K8) did not change with the loss of EGR4. (*H*) Circumvallate taste buds from *Egr4*$^{+/+}$ (*Top*) and *Egr4*$^{-/-}$ (*Bottom*) mice at P30 were immunolabeled with the antibodies to K8 (green) and NTPDASE2 (red). (*I*) Circumvallate taste buds from *Egr4*$^{+/+}$ (*Top*) and *Egr4*$^{-/-}$ (*Bottom*) mice at P30 were immunolabeled with antibodies to K8 (blue), TRPM5 (red), and CAR4 (green). (*J*) Total NTPDASE2+ pixels were significantly increased in circumvallate taste buds from the *Egr4*$^{-/-}$ mice compared to CV taste buds from *Egr4*$^{+/+}$ mice. (*K*) The total number of TRPM5+ taste bud cells, and (*L*) the percentage of the TRPM5+ taste bud cells were significantly reduced in the *Egr4*$^{-/-}$ mice compared to *Egr4*$^{+/+}$ mice. (*M*) The total number of CAR4+ taste bud cells, and (*N*) the percentage of the CAR4+ taste bud cells did not change due to the loss of EGR4. Error bars represent mean ± SEM; n = 5 mice analyzed. An unpaired *t* test with Welch's correction was used. **P* < 0.05, ***P* < 0.01, ****P* < 0.001, *****P* < 0.0001, ns = not significant. Scale bar is 25 μm for all images.

between *Egr4*$^{-/-}$ and *Egr4*$^{+/+}$ littermates (Fig. 6*H*). There were, however, significant decreases in nerve responses to sweet (sucrose) and umami (100 mM MPG+ 10 mM IMP) stimuli in *Egr4*$^{-/-}$ mice compared to *Egr4*$^{+/+}$ mice (Fig. 6 *A*, *C*, and *D*). In addition, there was no significant difference between *Egr4*$^{-/-}$ and *Egr4*$^{+/+}$ mice in CT responses to mechanical stimulation evoked by stroking of the anterior surface of the tongue (Fig. 6 *A* and *I*). Lastly, we did not observe any differences in the nerve responses to the application of NH_4Cl between mice of the different genotypes (Fig. 6 *A* and *J*). Taken together, these data indicate that EGR4 is necessary for the proper cell fate determination of GG neurons, specific taste cell maintenance, and sensory neuron responses to sweet and umami taste modalities.

EGR4 Deletion Alters the Expression of Axon Guidance Genes Resulting in a Significant Loss of Chemosensory Innervation of Taste Buds. To understand the molecular mechanisms by which EGR4 promotes the differentiation of GG neurons and the subsequent maintenance of TRPM5+ taste cells, a genome-wide transcriptome analysis was performed to identify differentially expressed genes in GG neurons collected from either *Egr4*$^{+/+}$ or *Egr4*$^{-/-}$ mice. Total mRNA samples were isolated from both GG pooled together from each mouse, and 4 mice of each genotype were analyzed. RNA was confirmed to be of high quality (RIN > 8) using a Bioanalyzer profile before conversion to cDNA libraries and sequencing (*SI Appendix*, Fig. S6 *A–C*). An average of 84.6% of the total reads obtained could be uniquely mapped to the mouse genome (mm10) generating an average of 57 million high-quality, mapped reads per sample (*SI Appendix*, Fig. S6*D*). Multidimensional scaling analysis was performed to compare the similarities between the RNA samples collected from individual mice (*SI Appendix*, Fig. S6*E*) and data from mice of each genotype clustered together, although there was some overlap between genotypes.

To broadly examine the enrichment and depletion of genes between groups, we performed DEG analysis on the *Egr4*$^{+/+}$ and *Egr4*$^{-/-}$ datasets. This analysis identified 29 genes by False Discovery Rate (FDR < 0.25) (**15 up-regulated, 14 down-regulated**) and **774** genes by *P* value (P < 0.05) (**322 up-regulated, 452 down-regulated**) that were significantly differentially expressed between the two genotypes. Volcano plots were generated from the data to identify global changes and trends in gene expression between *Egr4*$^{+/+}$ and *Egr4*$^{-/-}$ GG (Fig. 7 *A* and *B*). Gene set enrichment analysis (GSEA) was performed to identify the top 25 most up-regulated and top 25 most down-regulated genes that were differentially expressed between *Egr4*$^{+/+}$ and *Egr4*$^{-/-}$ GG neurons, and these data were depicted as heat maps (Fig. 7 *C* and *D*). These data were further analyzed for associated gene ontology (GO) using the hallmark gene dataset, and

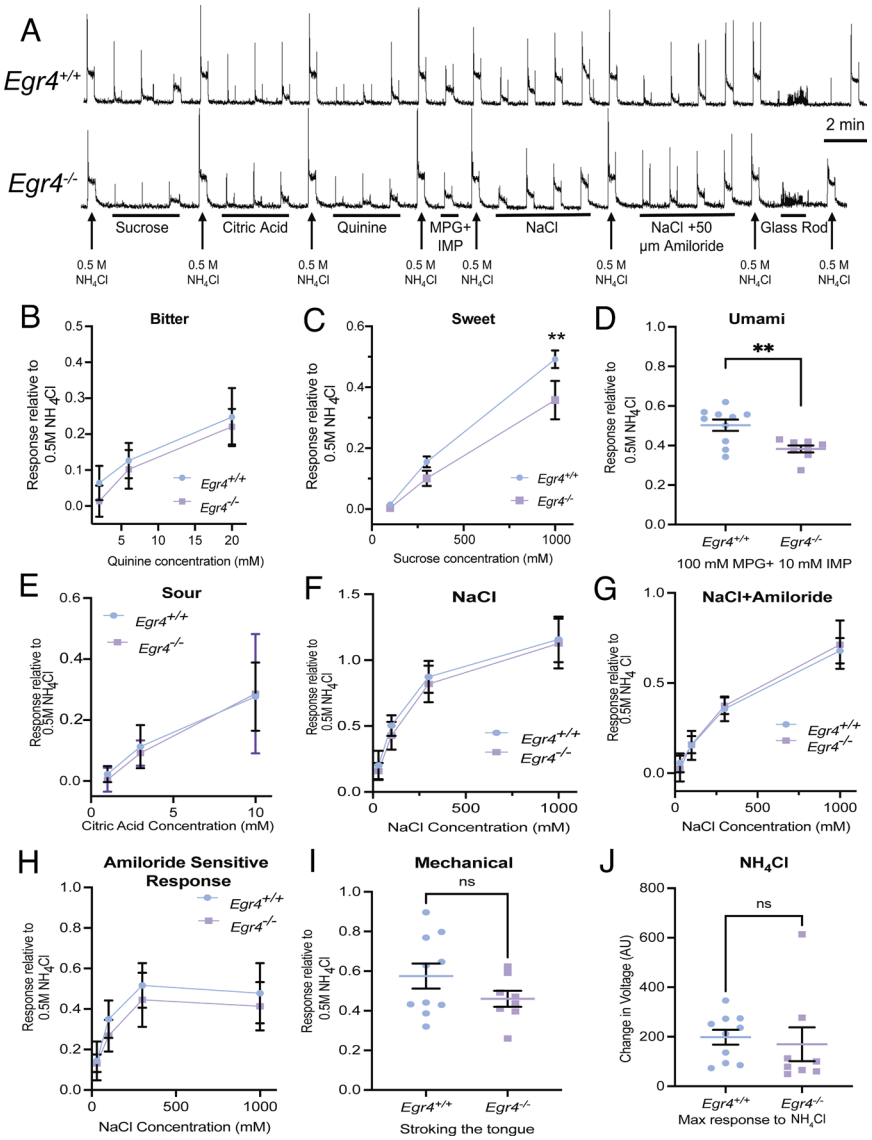

Fig. 6. Chorda Tympani responses to sweet and umami stimuli are reduced in *Egr4*$^{-/-}$ mice. (*A*) A representative example of integrated CT responses to chemical and tactile stimuli are shown for an *Egr4*$^{+/+}$ mouse (*Top* trace) and an *Egr4*$^{-/-}$ mouse (*Bottom* trace). Arrows display the presentation of 0.5 M NH_4Cl, which was used to normalize the data. Quantified stimulus-evoked responses are displayed for (*B*) the bitter stimulus quinine, (*C*) the sweet stimulus sucrose, (*D*) an umami mixture, (*E*) the sour stimulus citric acid, (*F*) the salty stimulus NaCl, and (*G*) NaCl mixed with 50 µM amiloride. (*H*) The amiloride-sensitive NaCl responses were calculated by deducting NaCl + amiloride values from responses to NaCl alone. (*I*) Peak integrated responses to gentle stroking of the tongue with a glass rod, and (*J*) changes in the voltage with NH_4Cl application were also analyzed. Error bars represent mean ± SEM, and n = 8 to 10 mice were analyzed for each experiment. Two-way ANOVA with Bonferroni's post hoc analysis and unpaired *t* tests with Welch's correction were used. **P* < 0.05, ***P* < 0.01, ****P* < 0.001, *****P* < 0.0001, ns = not significant.

the top 15 pathways that were either up-regulated or down-regulated were presented as a heat map (Fig. 7*E*).

Functionally grouped GO analysis of all up-regulated and down-regulated genes in *Egr4*$^{-/-}$ mice compared to *Egr4*$^{+/+}$ mice was performed using GENEONTOLOGY (35, 36). The top 5 up-regulated biological processes in *Egr4*$^{-/-}$ GG were mesangial cell development, folate import across plasma membrane, glomerulus vasculature development, myofibril assembly, and artery morphogenesis. Not surprisingly, the top 5 down-regulated biological processes were central nervous system myelination, semaphorin-plexin signaling pathway, positive regulation of axonogenesis, cholesterol biosynthetic process, and axon guidance (*SI Appendix*, Fig. S6*F*).

Consistent with our immunolabeling and FISH experiment, the RNA-seq analyses found that *P2rx2, Phox2b, Cdh4, and Spon1* were all significantly reduced in *Egr4*$^{-/-}$ GG, in addition to the purinergic receptor *P2rx3*. The RNA-seq data also revealed that three other GG neuron subpopulation markers, *Mafb, Ret,* and *Cdh13* were reduced in *Egr4*$^{-/-}$ mice, albeit these reductions were not significant (Dataset S1).

These analyses revealed that several genes that were most highly down-regulated in the *Egr4*$^{-/-}$ GG neurons, such as *Plxnb3*, *Draxin*, and *Robo2,* were axon guidance genes whose ligands (*Sema5a, Ntn1,* and *Slit,* respectively) are known to be expressed in taste cells (37, 38). We sought to validate the reduction in expression of these proteins in the GG via immunolabeling. As expected, expression of PLEXINB3, DRAXIN, ROBO2, and DCC were all down-regulated in GG neurons of *Egr4*$^{-/-}$ mice compared to *Egr4*$^{+/+}$ mice (Fig. 7*F*). Since EGR4 expression is limited to GG neurons and is not expressed in taste bud cells (*SI Appendix*, Fig. S7), we hypothesized that the significant reduction in chemosensory innervation of taste buds is caused by loss of axon guidance genes whose expression requires EGR4. To examine this, we collected anterior and posterior tongues and performed immunolabeling on fungiform and CV taste papillae. Interestingly, PLEXINB3, DCC, ROBO2, and DRAXIN were all selectively expressed in fibers entering taste buds, and this expression was significantly reduced in both fungiform and CV papillae of *Egr4*$^{-/-}$ mice (Fig. 7*G* for fungiform, and *SI Appendix*, Fig. S6*G* for CV). We also evaluated the expression of NETRIN-1, a ligand of DRAXIN, in taste bud cells as it was previously reported to be expressed in a small subset of taste cells (38). NETRIN-1 expression, which was expressed in taste bud cells, was also dramatically decreased in *Egr4*$^{-/-}$ mice. These data provide an explanation of how the loss of EGR4 may lead to the loss of chemosensory innervation of

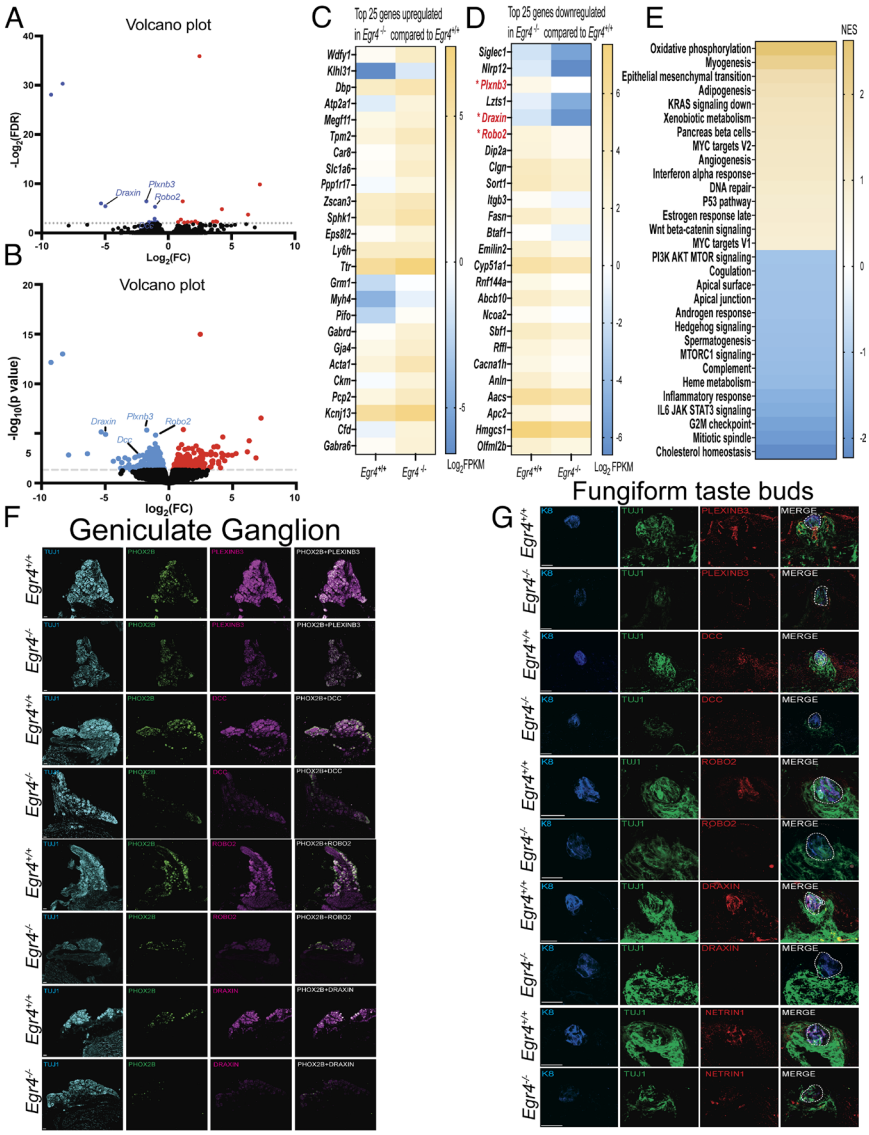

Fig. 7. *Egr4* deletion significantly alters the expression of axon guidance genes in both GG and the CT nerve terminals present in fungiform taste buds. (*A*) Volcano plot identifying the differentially expressed genes by FDR between $Egr4^{+/+}$ and $Egr4^{-/-}$ GG neurons with axon guidance genes labeled in the plot. (*B*) Volcano plot identifying the differentially expressed genes by *P* value between $Egr4^{+/+}$ and $Egr4^{-/-}$ GG neurons with axon guidance genes indicated in the plot. For both Figures *A* and *B*, the down-regulated genes were marked in blue and the up-regulated genes are marked in red. (*C*) Heat map showing the top 25 genes that were up-regulated according to GSEA. (*D*) Heat map showing the top 25 most down-regulated genes identified by the GSEA analysis. Down-regulated axon guidance genes are marked in red in the heat map. (*E*) GSEA pathway analysis was performed to identify hallmark signaling pathways that were significantly increased (yellow) or decreased (blue) in the GG of $Egr4^{-/-}$ mice compared to the $Egr4^{+/+}$ mice. (*F*) To confirm the expression of the down-regulated axon guidance genes identified in the GG by RNA-seq, we performed immunolabeling in GG sections. GG neurons were stained with the pan-neuronal marker TUJ1 (cyan), oral sensory neuron marker PHOX2B (green), and the four axon guidance proteins PLEXINB3, DCC, ROBO2, and DRAXIN (all magenta) from *Top* to *Bottom*, respectively. In each pair of rows of panels, the *Top* panels are from $Egr4^{+/+}$ mice, and the *Bottom* panels are from $Egr4^{-/-}$ mice. (*G*) Expression of these axon guidance proteins was evaluated in the axon terminals innervating fungiform taste buds. Fungiform taste buds were labeled with the taste cell marker K8 (blue), pan-neuronal marker TUJ1 (green), and the four axon guidance proteins PLEXINB3, DCC, ROBO2, and DRAXIN (all red), from *Top* to *Bottom*. We also evaluated the expression of the ligand of the DRAXIN-DCC complex, NETRIN1, in the taste cells. In each pair of the rows, the *Top* panels are from $Egr4^{+/+}$ mice, and the *Bottom* panels are from $Egr4^{-/-}$ mice. n = 3 to 4 mice were analyzed. Scale bar is 25 μm for all images.

taste buds and TRPM5+ taste cells, namely by axon guidance and synaptogenesis impairments.

Discussion

The presence of oral sensory and pinna-innervating somatosensory neurons within the same ganglia, each with specific transcription factor requirements and central projections, makes the GG an interesting structure to study neuronal cell fate determination and maintenance. The time course expression data using both FISH and immunolabeling support the conclusion that EGR4 is not required for the initiation of PHOX2B expression which occurs as early as E12.5 (39, 40) but is critical for the postnatal cell-fate determination and maintenance of the oral sensory phenotype of GG neurons. Results from the evaluation of $Egr4^{-/-}$ mice indicate that EGR4 is not required for neuronal survival, even though its deletion caused a significant loss of oral sensory PHOX2B+ cells, simultaneously shifting these neurons to expressing BRN3A, revealing EGR4's critical role in maintaining PHOX2B expression after birth. A previous study examining $Phox2b^{LacZ/LacZ}$ knockout mice demonstrated that a loss of PHOX2B expression leads to the acquisition of a BRN3A+ somatosensory phenotype (6). In cranial ganglia, BRN3A expression and the associated somatosensory fate is likely the default phenotype, whereas the initiation of PHOX2B expression represses BRN3A leading to the transition to an oral sensory phenotype (6). This type of molecular switch between somatosensory and visceral fates has been reported in trigeminal ganglia and in the nucleus of solitary tract in hindbrain (41, 42). Our data suggest that EGR4 acts as the postnatal molecular pathway that maintains PHOX2B expression, also driving further differentiation into specific subtypes of oral sensory neurons. Since EGR4 deletion does not lead to a complete loss of PHOX2B expression in oral sensory neurons, it is evident that either EGR4 acts in combination with other transcriptional regulators or that other transcription factors maintain PHOX2B expression in the remaining oral sensory neurons independently of EGR4.

While all PHOX2B+ oral sensory neurons in GG express EGR4 protein, *Egr4* mRNA expression can be grouped into two populations of roughly equal sizes, one expressing a high-level *Egr4* mRNA and the other expressing low *Egr4*. Because the loss of *Egr4* causes an approximately 50% loss of PHOX2B+ neurons and 50% loss of taste bud innervation, this suggests that EGR4's important roles in phenotypic maintenance are only in the high *Egr4*-expressing PHOX2B+ neurons. Therefore, in the low *Egr4*-expressing neurons, either this level of Egr4 is not sufficient to drive differentiation of these neurons and some other pathway does or, alternatively,

additional transcription factors and/or coregulators also contribute and compensate for the loss of Egr4, as speculated above. On the other hand, it is also possible that the low *Egr4*-expressing neurons are the ones impaired by *Egr4* deletion. Regardless, the results reported here are not able to distinguish between these possibilities and will require a deep investigation of the transcriptional machinery active in developing GG neurons.

The observation that *Egr4* expression in GG neurons does not begin before P7 raises the question of what signaling pathways induce *Egr4* expression. Previous studies have shown that BDNF, acting via its receptor TRKB, is critically important for GG oral sensory neuron survival, target innervation, and maintenance (43–46). This raises the possibility that TRKB-BDNF signaling activates EGR4 expression and signaling in GG neurons, especially considering that BDNF promotes EGR4 expression in hippocampal neurons (47). Another study demonstrated that neurturin, via its receptors *Ret* and *GFRα2,* activates the MAPK pathway to modulate *Egr4* function (48). Interestingly, *Neurturin* was one of the genes that was up-regulated in $Egr4^{-/-}$ GG compared to $Egr4^{+/+}$ in the RNA-seq analysis, suggesting there may be feedback mechanisms working between these pathways.

Oral sensory neurons of GG are a diverse population of neurons that transduce several types of sensory information including taste, touch, and temperature. Just recently have these subpopulations of GG oral sensory neurons that convey specific sensory modalities begun to be described molecularly (7–9). Indeed, our understanding of cellular diversification from a homogenous PHOX2B+ oral sensory neuron population is rudimentary compared to other peripheral ganglia, such as the DRG (49). Our findings indicate that *Egr4* plays a key role in the process since we observed significant losses in *Ret*/MAFB, *Cdh13*, and FOXG1-expressing subpopulations of GG oral sensory neurons but not *Penk*-expressing sour-responsive neurons.

Importantly, *Egr4* deletion caused significant loss of both fungiform and CV taste buds, as well as their innervation, starting at P7. We observed that some fungiform papillae retain their normal structure but lack a taste bud altogether. These papillae can be best described as atypical papillae (21, 50) and were more numerous in $Egr4^{-/-}$ mice. Several studies indicate that the maintenance of taste buds is dependent on the *Shh/Gli* signaling pathway (21, 51). Interestingly, Hedgehog signaling was in the top ten most down-regulated pathways in GG from the RNA-seq analysis of $Egr4^{-/-}$ mice compared to $Egr4^{+/+}$ mice, and we cannot rule out the possibility of disruption of the *Shh/Gli* pathway in the taste epithelium of $Egr4^{-/-}$ mice.

Loss of EGR4 prominently impaired chemosensory innervation of postnatal taste buds starting from P7, the same time EGR4 begins to be expressed in GG neurons. TUJ1 (b-Tubulin) is expressed specifically in neurons and forms the essential microtubule network implicated in neurogenesis, axon guidance, and maintenance. Loss of TUJ1 and associated microtubule disorganization is associated with axonal retraction (52, 53) which is similar to the phenotype seen here. P2X3 expression is also lost in the taste bud innervating fibers in $Egr4^{-/-}$ mice. While it is possible that these innervating fibers could still be present to some degree and just devoid of TUJ1 and P2X3 labeling, they would likely have cytoskeletal abnormalities and impaired responses to ATP release.

Further investigation into the loss of K8 revealed a reduction in TRPM5-expressing type II taste cells, with a concomitant increase in NTPDASE2+ type I cells. While it is possible that TRPM5 expression is lost but these cells remain otherwise normal, the appearance of increased numbers of NTPDASE2-expressing cells raise the possibility that there is a shift in differentiation from type II to type I cells. It is unclear, however, whether these TRPM5+ cells in $Egr4^{-/-}$ mice degenerate more rapidly, or whether they dedifferentiate and then adopt a type I cell fate. Another possibility is that innervation from EGR4-dependent GG neurons is necessary for the formation of a subset of type II cells, and without this input, those receptor cells do not form. Interestingly, taste bud area declined in fungiform papillae in $Egr4^{-/-}$ mice, suggesting a loss of cells, but not in CV taste buds. Future studies are necessary to evaluate how EGR4-expressing GG neurons control the maintenance and/or differentiation of taste receptor cells, and whether subsets of TRPM5-expressing type II cells are affected differentially. Interestingly, SEMA3A and SEMA7A are reported to provide critical instructive cues for the communication between taste bud cells and taste neurons (54). Our study identifies other axon guidance molecule receptors, namely PLEXINB3, DCC, ROBO2, and DRAXIN, as potentially critical for taste bud innervation. This points to a possible model of taste receptor cell maintenance in which a transcription factor, expressed in GG neurons, controls axon guidance receptor complex expression that in turn promotes selective taste receptor cell innervation and taste cell maintenance.

Consistent with the loss of TRPM5+ type II taste cells and loss of chemosensory innervation, CT nerve responses to sweet and umami stimuli were significantly reduced. Surprisingly, bitter responses were not altered. Because some TRPM5-expressing cells persist in $Egr4^{-/-}$ mice, it is possible that these cells are bitter-responsive type II cells. Also, a subset of type III cells has been implicated in the detection of bitter (55, 56), and it is possible that they are compensating in the bitter responses, given that type III cells were not altered in $Egr4^{-/-}$ mice. In conclusion, the data presented here identify EGR4 as a critical regulator of postnatal cell-fate determination of GG neurons and is subsequently required for taste bud innervation and the maintenance of TRPM5-expressing taste receptor cells necessary for sweet and umami. The remarkable phenotypic changes that occur in GG and taste buds subsequent to EGR4 disruption suggests that plasticity within peripheral taste circuits could be therapeutically relevant for those suffering from taste impairments.

Experimental Model and Subject Details

Animals. All experiments were performed in compliance with the guidelines of the American Association for Accreditation of Laboratory Animal Care (AAALAC) and were approved by the Institutional Animal Care and Use Committee of the Indiana University School of Medicine. Postnatal day 30 (P30) $Egr4^{-/-}$ ($Egr4^{tm1Jmi}/Egr4^{tm1Jmi}$) mice (RRID: MGI:2658746) (26) and their wild-type littermates ($Egr4^{+/+}$) were used for these experiments unless mentioned otherwise. For the developmental time course experiments, postnatal day 3 (P3), postnatal day 7 (P7), postnatal day 10 (P10), and postnatal day 30 (P30) $Egr4^{+/+}$ were used. The $Egr4^{-/-}$ mice were generously provided by Jonathan Soboloff, Temple University School of Medicine, and Dr. Warren Tourtellotte, Cedars Sinai Medical Center.

FISH. Mice were killed and transcardially perfused, and GG was collected and cryopreserved. Then, 20 μm sections of the GG were cut and then subjected to FISH analysis. The following probes were used: *Egr4* (553851-C1), *Phox2b* (407861-C2), *Brn3a* (*Pou4f1*) (414671-C3), *Ret* (431791-C1), *Cdh13* (443251-C1), *Penk* (318761-C3), *Cdh4* (534651-C3), and *Spon1*(401991-C1) (Advanced Cell Diagnostics). Further details are provided in SI Materials and Methods.

Immunolabeling. Tissues were collected as just described for FISH. For Immunolabeling experiments, GG, nodose/petrosal ganglia, and the anterior tongue containing fungiform papillae were sectioned at 20 μm and mounted onto precleaned slides. The posterior tongue

containing circumvallate papillae was sectioned at 50 µm, and immunolabeling was done in free-floating sections. Further details and antibodies used are provided in *SI Appendix, Materials and Methods*.

Image Collection. The images were collected using a SP8 Lightning confocal microscope (Leica Microsystems) with LAS-X software. High-resolution (2,048 × 2,048) Z-stack images were captured using an optical step size of 1 µm at either 20× or 63× magnifications. Images were only adjusted for brightness and contrast.

Quantification of Geniculate Ganglion Neurons, Taste Papillae, and Taste Bud Innervation. Intact GGs were collected, cryosectioned (20 µm), imaged, and processed as described above. The number of neurons was counted through each Z-stack section such that neurons were not counted more than once. All sections containing the GG were counted and added together to determine the total number of neurons in the entire ganglion. Further details are provided in *SI Appendix*, Materials and Methods.

Z-stacks were collected using confocal imaging such that fungiform and circumvallate papillae were captured in their entirety. After collecting the images, the data were imported into ImageJ (RRID:SCR_003070) using the Fiji image-processing package (RRID:SCR_002285) (57). The total number of taste buds (identified by K8 labeling) was counted by evaluating the entire papilla captured on serial sections. Typically, ten taste buds from each tongue were measured, and they were evenly distributed throughout the tongue. All TUJ1+ and P2X3+ pixels in taste papilla regions were quantified by the software. Further details are provided in *SI Appendix, Materials and Methods*.

CT Nerve Recordings. Mice were anesthetized with urethane and the CT was exposed via the mandibular approach. The nerve was cut and placed on a platinum wire electrode, and a copper electrode was clipped onto nearby muscle. Signals were recorded with Spike 2 software (Cambridge Electronic Design) and integrated digitally using a time constant of 0.5 s. To evoke tactile responses, a glass rod was brushed across the tongue. The peak integrated response was averaged across tactile stimulations. For taste stimuli, baseline activity was subtracted from steady-state activity and this change in activity was normalized to the change in response to 500 mM ammonium chloride (NH_4Cl) which was applied before and after each type of stimulus. Further details are provided in *SI Appendix, Materials and Methods*.

RNA Extraction, cDNA Library Preparation, RNA-seq, and RNA-seq Data Analysis. Total RNA was extracted from isolated GG from four *Egr4*$^{+/+}$ and four *Egr4*$^{-/-}$ mice each using the RNeasy plus micro kit (Qiagen, catalog no. 74034) according to the manufacturer's instructions. Equal numbers of male and female mice were analyzed (two males and two females of each genotype). One nanogram of total RNA was used for library preparation using the Clontech SMART-Seq v4 Ultra Low Input RNA Kit (Takara Bio USA, Inc.) and the Illumina Nextera XT DNA Library Kit (Illumina). The pooled libraries were sequenced on an Illumina NovaSeq 6000 sequencer. The sequence data have been deposited into the Gene Expression Omnibus (GEO) repository under the accession number GSE223724 (58).

The sequencing reads were first quality checked using FastQC (v.0.11.5, Babraham Bioinformatics, Cambridge, UK). The sequence data were then mapped to the mouse reference genome mm10 using the RNA-seq aligner STAR (v.2.5) (59). Differential expression analysis was performed using edgeR (v.3.12.1) (60, 61). A ranked gene list was generated based on the differential gene expression analysis, and the list was used for gene set enrichment analysis with GSEA (https://www.gsea-msigdb.org/gsea/index.jsp). The gene set from Molecular Signatures Database (MSigDB) was applied for the GSEA analysis: H1 (Hallmark gene sets). GO analysis was performed using http://geneontology.org/. All the up-regulated and down-regulated genes were analyzed for three different criteria: 1) cellular component, 2) molecular function, and 3) biological process. Further details are provided in *SI Appendix, Materials and Methods*.

Statistical Analysis. All statistical analyses were performed using Prism 9 software (GraphPad). Before analysis, data were evaluated for normal distribution using the Shapiro–Wilk test and were determined to be normally distributed at $P < 0.05$. Accordingly, Welch's *t* test and one- or two-way ANOVA were used for all analyses. Significant differences among pairwise comparisons were identified by Bonferroni's post hoc tests. All graphs and error bars represent the mean ± SEM. The details on sample sizes (n) are included in the figure legends, and extent of significance is $^{*}P < 0.05$, $^{**}P < 0.01$, $^{***}P < 0.001$, $^{****}P < 0.0001$, which is also included in the Figure Legends.

Data, Materials, and Software Availability. Sequence data have been deposited in NCBI Gene Expression Omnibus (GSE223724) (58). All study data are included in the article and/or *SI Appendix*.

ACKNOWLEDGMENTS. We thank Dr. Kathryn Medler for providing valuable comments on the manuscript. We also thank Ed Simpson, Makshita Luthra, Hongyu Gao, and Xiaoling Xuei for technical support in analyzing the RNA-seq data. Catherine Kaminski and Wesley Stansberry provided technical assistance and helpful suggestions. This work was supported by a National Institute on Deafness and Other Communication Disorders grant R01 DC015799 to B.A.P.

Author affiliations: [a]Department of Anatomy, Cell Biology & Physiology, Stark Neurosciences Research Institute, Indiana University School of Medicine, Indianapolis, IN 46202; [b]Department of Cancer & Cellular Biology, Fels Cancer Institute for Personalized Medicine, Lewis Katz School of Medicine at Temple University, Philadelphia, PA 19140; and [c]Department of Pathology and Laboratory Medicine, Neurology, and Neurological Surgery, Cedars-Sinai Medical Center, Los Angeles, CA 90048

1. Y. Liu, Q. Ma, Generation of somatic sensory neuron diversity and implications on sensory coding. *Curr. Opin. Neurobiol.* **21**, 52–60 (2011).
2. I. M. Dykes, L. Tempest, S. I. Lee, E. E. Turner, Brn3a and Islet1 act epistatically to regulate the gene expression program of sensory differentiation. *J. Neurosci.* **31**, 9789–9799 (2011).
3. F. Lallemend, P. Ernfors, Molecular interactions underlying the specification of sensory neurons. *Trends Neurosci.* **35**, 373–381 (2012).
4. D. M. Lopes, F. Denk, S. B. McMahon, The molecular fingerprint of dorsal root and trigeminal ganglion neurons. *Front. Mol. Neurosci.* **10**, 304 (2017).
5. M. Yoshikawa *et al.*, Runx1 selectively regulates cell fate specification and axonal projections of dorsal root ganglion neurons. *Dev. Biol.* **303**, 663–674 (2007).
6. F. D'Autreaux, E. Coppola, M. R. Hirsch, C. Birchmeier, J. F. Brunet, Homeoprotein Phox2b commands a somatic-to-visceral switch in cranial sensory pathways. *Proc. Natl. Acad. Sci. U.S.A.* **108**, 20018–20023 (2011).
7. C. R. Donnelly, A. A. Shah, C. M. Mistretta, R. M. Bradley, B. A. Pierchala, Biphasic functions for the GDNF-Ret signaling pathway in chemosensory neuron development and diversification. *Proc. Natl. Acad. Sci. U.S.A.* **115**, E516–E525 (2018).
8. G. Dvoryanchikov *et al.*, Transcriptomes and neurotransmitter profiles of classes of gustatory and somatosensory neurons in the geniculate ganglion. *Nat. Commun.* **8**, 760 (2017).
9. J. Zhang *et al.*, Sour sensing from the tongue to the brain. *Cell* **179**, 392–402.e15 (2019).
10. I. Perea-Martinez, T. Nagai, N. Chaudhari, Functional cell types in taste buds have distinct longevities. *PLoS One* **8**, e53399 (2013).
11. T. Okubo, C. Clark, B. L. Hogan, Cell lineage mapping of taste bud cells and keratinocytes in the mouse tongue and soft palate. *Stem Cells* **27**, 442–450 (2009).
12. M. Ohmoto *et al.*, Genetic lineage tracing in taste tissues using Sox2-CreERT2 strain. *Chem. Senses* **42**, 547–552 (2017).
13. J. M. D. Olmsted, Effects of cutting the lingual nerve of the dog. *J. Comp. Neurol.* **33**, 149–154 (1921), 10.1002/cne.900330204.
14. J. H. M. Vintschgau, J. Honigschmied, Nervus Glossopharyngeus und Schmeckbecher. *Archiv für die gesamte Physiologie des Menschen und der Tiere.* **14**, 443–448 (1877), 10.1007/BF01635485.
15. M. A. Hosley, S. E. Hughes, B. Oakley, Neural induction of taste buds. *J. Comp. Neurol.* **260**, 224–232 (1987).

16. M. A. Hosley, S. E. Hughes, L. L. Morton, B. Oakley, A sensitive period for the neural induction of taste buds. *J. Neurosci.* **7**, 2075–2080 (1987).
17. M. Cheal, B. Oakley, Regeneration of fungiform taste buds: temporal and spatial characteristics. *J. Comp. Neurol.* **172**, 609–626 (1977).
18. L. Guth, Taste buds on the cat's circumvallate papilla after reinnervation by glossopharyngeal, vagus, and hypoglossal nerves. *Anat. Rec.* **130**, 25–37 (1958).
19. W. J. Lu *et al.*, Neuronal delivery of Hedgehog directs spatial patterning of taste organ regeneration. *Proc. Natl. Acad. Sci. U.S.A.* **115**, E200–E209 (2018).
20. X. Lin *et al.*, R-spondin substitutes for neuronal input for taste cell regeneration in adult mice. *Proc. Natl. Acad. Sci. U.S.A.* **118**, e2001833118 (2021).
21. A. N. Ermilov *et al.*, Maintenance of taste organs is strictly dependent on epithelial Hedgehog/GLI signaling. *PLoS Genet.* **12**, e1006442 (2016).
22. E. Sanz *et al.*, Cell-type-specific isolation of ribosome-associated mRNA from complex tissues. *Proc. Natl. Acad. Sci. U.S.A.* **106**, 13939–13944 (2009).
23. J. L. Shadrach *et al.*, Translatomic analysis of regenerating and degenerating spinal motor neurons in injury and ALS. *iScience* **24**, 102700 (2021).
24. C. M. Mistretta, K. A. Goosens, I. Farinas, L. F. Reichardt, Alterations in size, number, and morphology of gustatory papillae and taste buds in BDNF null mutant mice demonstrate neural dependence of developing taste organs. *J. Comp. Neurol.* **409**, 13–24 (1999).
25. R. F. Krimm, Factors that regulate embryonic gustatory development. *BMC Neurosci.* **8** (suppl. 3), S4 (2007).
26. W. G. Tourtellotte, R. Nagarajan, A. Auyeung, C. Mueller, J. Milbrandt, Infertility associated with incomplete spermatogenic arrest and oligozoospermia in Egr4-deficient mice. *Development* **126**, 5061–5071 (1999).
27. E. J. Huang *et al.*, Brn3a is a transcriptional regulator of soma size, target field innervation and axon pathfinding of inner ear sensory neurons. *Development* **128**, 2421–2432 (2001).
28. D. Dutta Banik, K. F. Medler, Taste receptor signaling. *Handb. Exp. Pharmacol.* **275**, 33–52 (2021), 10.1007/164_2021_442.
29. R. G. Murray, A. Murray, S. Fujimoto, Fine structure of gustatory cells in rabbit taste buds. *J. Ultrastruct. Res.* **27**, 444–461 (1969).
30. R. G. Murray, Cellular relations in mouse circumvallate taste buds. *Microsc. Res. Tech* **26**, 209–224 (1993).
31. D. L. Bartel, S. L. Sullivan, E. G. Lavoie, J. Sevigny, T. E. Finger, Nucleoside triphosphate diphosphohydrolase-2 is the ecto-ATPase of type I cells in taste buds. *J. Comp. Neurol.* **497**, 1–12 (2006).
32. D. Dutta Banik, L. E. Martin, M. Freichel, A. M. Torregrossa, K. F. Medler, TRPM4 and TRPM5 are both required for normal signaling in taste receptor cells. *Proc. Natl. Acad. Sci. U.S.A.* **115**, E772–E781 (2018).
33. Z. Zhang, Z. Zhao, R. Margolskee, E. Liman, The transduction channel TRPM5 is gated by intracellular calcium in taste cells. *J. Neurosci.* **27**, 5777–5786 (2007).
34. J. Chandrashekar *et al.*, The taste of carbonation. *Science* **326**, 443–445 (2009).
35. M. Ashburner *et al.*, Gene ontology: Tool for the unification of biology. The Gene Ontology Consortium. *Nat. Genet.* **25**, 25–29 (2000).
36. C. Gene Ontology, The Gene Ontology resource: Enriching a GOld mine. *Nucleic Acids Res.* **49**, D325–D334 (2021).
37. J. Shandilya, Y. Gao, T. K. Nayak, S. G. Roberts, K. F. Medler, AP1 transcription factors are required to maintain the peripheral taste system. *Cell Death Dis.* **7**, e2433 (2016).
38. S. K. Sukumaran *et al.*, Whole transcriptome profiling of taste bud cells. *Sci. Rep.* **7**, 7595 (2017).
39. S. Dauger *et al.*, Phox2b controls the development of peripheral chemoreceptors and afferent visceral pathways. *Development* **130**, 6635–6642 (2003).
40. A. Pattyn, X. Morin, H. Cremer, C. Goridis, J. F. Brunet, Expression and interactions of the two closely related homeobox genes Phox2a and Phox2b during neurogenesis. *Development* **124**, 4065–4075 (1997).
41. E. J. Kim, J. Battiste, Y. Nakagawa, J. E. Johnson, Ascl1 (Mash1) lineage cells contribute to discrete cell populations in CNS architecture. *Mol. Cell Neurosci.* **38**, 595–606 (2008).
42. M. A. Sieber *et al.*, Lbx1 acts as a selector gene in the fate determination of somatosensory and viscerosensory relay neurons in the hindbrain. *J. Neurosci.* **27**, 4902–4909 (2007).
43. D. Fei, R. F. Krimm, Taste neurons consist of both a large TrkB-receptor-dependent and a small TrkB-receptor-independent subpopulation. *PLoS One* **8**, e83460 (2013).
44. T. Huang, L. Ma, R. F. Krimm, Postnatal reduction of BDNF regulates the developmental remodeling of taste bud innervation. *Dev. Biol.* **405**, 225–236 (2015).
45. L. Meng, L. Ohman-Gault, L. Ma, R. F. Krimm, Taste bud-derived bdnf is required to maintain normal amounts of innervation to adult taste buds. *eNeuro* **2**, ENEURO.0097-15.2015 (2015).
46. T. Tang, J. Rios-Pilier, R. Krimm, Taste bud-derived BDNF maintains innervation of a subset of TrkB-expressing gustatory nerve fibers. *Mol. Cell Neurosci.* **82**, 195–203 (2017).
47. A. Ludwig *et al.*, Early growth response 4 mediates BDNF induction of potassium chloride cotransporter 2 transcription. *J. Neurosci.* **31**, 644–649 (2011).
48. A. Ludwig *et al.*, Neurturin evokes MAPK-dependent upregulation of Egr4 and KCC2 in developing neurons. *Neural. Plast.* **2011**, 1–8 (2011).
49. S. Meltzer, C. Santiago, N. Sharma, D. D. Ginty, The cellular and molecular basis of somatosensory neuron development. *Neuron* **109**, 3736–3757 (2021).
50. A. Kumari *et al.*, Recovery of taste organs and sensory function after severe loss from Hedgehog/Smoothened inhibition with cancer drug sonidegib. *Proc. Natl. Acad. Sci. U.S.A.* **114**, E10369–E10378 (2017).
51. C. M. Mistretta, A. Kumari, Hedgehog signaling regulates taste organs and oral sensation: Distinctive roles in the epithelium, stroma, and innervation. *Int. J. Mol. Sci.* **20**, 1341 (2019).
52. A. Erturk, F. Hellal, J. Enes, F. Bradke, Disorganized microtubules underlie the formation of retraction bulbs and the failure of axonal regeneration. *J. Neurosci.* **27**, 9169–9180 (2007).
53. Y. He, W. Yu, P. W. Baas, Microtubule reconfiguration during axonal retraction induced by nitric oxide. *J. Neurosci.* **22**, 5982–5991 (2002).
54. H. Lee, L. J. Macpherson, C. A. Parada, C. S. Zuker, N. J. P. Ryba, Rewiring the taste system. *Nature* **548**, 330–333 (2017).
55. D. Dutta Banik *et al.*, A subset of broadly responsive Type III taste cells contribute to the detection of bitter, sweet and umami stimuli. *PLoS Genet.* **16**, e1008925 (2020).
56. D. Dutta Banik, K. F. Medler, Bitter, sweet, and umami signaling in taste cells: It's not as simple as we thought. *Curr. Opin. Physiol.* **20**, 159–164 (2021).
57. J. Schindelin *et al.*, Fiji: An open-source platform for biological-image analysis. *Nat. Methods* **9**, 676–682 (2012).
58. D. D. Banik, B. A. Pierchala, EGR4 is critical for cell-fate determination and maintenance of Geniculate Ganglion neurons underlying sweet and umami taste. https://www.ncbi.nlm.nih.gov/geo/query/acc.cgi?acc=GSE223724. Deposited 25 January 2023.
59. A. Dobin *et al.*, STAR: Ultrafast universal RNA-seq aligner. *Bioinformatics* **29**, 15–21 (2013).
60. D. J. McCarthy, Y. Chen, G. K. Smyth, Differential expression analysis of multifactor RNA-Seq experiments with respect to biological variation. *Nucleic Acids Res.* **40**, 4288–4297 (2012).
61. M. D. Robinson, D. J. McCarthy, G. K. Smyth, edgeR: A Bioconductor package for differential expression analysis of digital gene expression data. *Bioinformatics* **26**, 139–140 (2010).